URSI GASS 2021, Rome, Italy, 28 August - 4 September 2021

Analysis of the Influence of Mars Ionosphere on Tianwen 1 Subsurface Detection Radar Imaging URSI Summary Paper Template

Longxiang Wang[(1)], Hongxia Ye[(2)]
(1) Key Laboratory of EMW Information, Fudan University, Shanghai, China
(2) Key Laboratory of EMW Information, Fudan University, Shanghai, China

Abstract

On July 23, 2020, China's self-developed Mars rover Tianwen 1 successfully launched into space. In order to study the impact of the Martian ionosphere on the imaging of the Orbiter Subsurface Investigation Radar carried by the Tianwen 1, this paper derives the deviation of the one-dimensional and two-dimensional chirp signals of the Tianwen 1 radar under Mars ionospheric electron densities. From the simulation results, it can be seen that due to the low working frequency of the subsurface radar on the Tianwen 1 track, after pulse compression, it will produce a positive offset and defocus along the range in the range, and the maximum offset in the case of 10TECU reach 23.96 meters, defocus seriously and the lower the operating frequency band, the more serious the offset and defocus.

1 Introduction

Mars is the most similar planet among all planets in the solar system. So far, mankind has made more than 40 exploration attempts on the earth, among which the more successful are the Mars Advanced Radar for Subsurface and Ionosphere Sounding (MARSIS) launched by ESA in 2003 and the Shallow Subsurface Radar (SHARAD) launched by NASA [1]. China also successfully launched the Mars rover Tianwen 1 on July 3, 2020. The rover and orbiter on the rover are equipped with subsurface detection radars. The subsurface detection radar can penetrate the surface of Mars by emitting low-frequency, electromagnetic waves, thereby detecting the surface and underground of Mars. The Tianwen 1 Mars Orbiter Subsurface Investigation Radar (MOSIR) performs azimuth processing on the satellite, and then performs range processing on the ground. Due to the low working frequency of the orbital subsurface detection radar, the frequency range is 10-50MHz, which is greatly affected by the Martian ionosphere. The ionosphere has a great influence on the time delay, amplitude and phase of the Martian surface echo. During the pulse compression process, there will be unbalanced matching, resulting in blurred images. MARSIS uses the contrast method to correct the ionosphere [2], which is based on the phase estimation of the influence of the total electron density of the electromagnetic wave passing through the ionosphere on the echo, thereby compensating the phase of the echo. SHARAD uses the phase gradient autofocus algorithm (PGA) to estimate the phase error based on the strong scattering points in the echo, and calculate the azimuth ionospheric additional phase for phase compensation [3]. In this paper, the influence of the Martian ionosphere on the imaging of Tianwen 1 is analyzed, compared the displacement and defocus of the one-dimensional point target in the range of different TEC conditions, and simulated and analyzed the impact of the ionosphere to the two-dimensional point target.

2 The influence of the stationary ionosphere on the Orbiter Subsurface Investigation Radar of Tianwen 1

The refractivion index of electromagnetic waves passing through the ionosphere is determined by frequency and electric density [4].

$$n(f) \approx 1 + \frac{A}{f^2} N_e \quad (1)$$

Here f is the frequency of transmitting signal, N_e is the electron density in m^{-3}, A=40.28 m^3/s^2 is a constant of ionosphere. Then the time delay of receiving signal can be calculated.

$$t(f) = \frac{1}{c}\int_{\text{path}} [n(f)-1]ds = \frac{A}{cf^2}\int_{\text{path}} N_e ds = \frac{A}{cf^2} TEC \quad (2)$$

Where TEC is the total electron content in the path of electromagnetic waves. According to the relationship between time and phase, the phase delay of the round-trip signal can be calculated as.

$$\Delta\phi(f) = 4\pi f t(f) = \frac{4\pi \cdot A}{cf} TEC = \frac{4\pi \cdot A}{c(\Delta f + f_0)} TEC \quad (3)$$

Where Δf is the band and f_0 is the carrier frequency of radar signal. The Taylor expansion of Eq. (3) can get the phase expansion as following [5].

$$\Delta\phi(f) \approx \Delta\phi_0(f) + \Delta\phi_1(f) + \Delta\phi_2(f) + \Delta\phi_3(f) \quad (4)$$

$$\Delta\phi_0(f) = -\frac{4\pi A \cdot TEC}{cf_0}$$
$$\Delta\phi_1(f) = \frac{4\pi A \cdot TEC}{cf_0^2} f$$
$$\Delta\phi_2(f) = -\frac{4\pi A \cdot TEC}{cf_0^3} f^2 \tag{5}$$
$$\Delta\phi_3(f) = \frac{2\pi A \cdot TEC}{cf_0^4} f^3$$

Here $\Delta\phi_1(f), \Delta\phi_2(f), \Delta\phi_3(f)$ represent the constant, linear, quadratic and cubic phase error about frequency respectively. Subsurface detection radar emits chirp pulses at a fixed period. For a point target, the range resolution is determined by the pulse width, and the azimuth resolution is determined by the length of the synthetic aperture. Suppose the radar transmission sequence is continuous pulse.

$$s(t) = \sum_{n=-\infty}^{\infty} p(t - n \cdot PRT)$$
$$p(t) = rect(\frac{t}{Tr}) e^{j\pi K_r t^2} e^{j2\pi f_0 t} \tag{6}$$

Where *rect* represents a rectangular signal, K_r is the FM slope of range chirp signal, PRT is the pulse repetition time of the pulse, f_0 is the carrier frequency of radar signal. The radar echo signal is determined by the transmitted signal waveform, antenna pattern, slant distance, Mars surface RCS, environment and other factors. If environmental factors are not considered, the single-point target radar echo signal can be written as.

$$S_r(t) = \sum_{n=-\infty}^{\infty} \sigma \cdot w \cdot \mathrm{p}(t - n \cdot \mathrm{PRT} - \tau_n) \tag{7}$$

Where σ is the radar cross section of the point target, w represents the two-way amplitude weighting of the antenna pattern of the point target, and τ_n represents the round-trip time of electromagnetic wave propagation between the radar and the target when the aircraft transmits the nth pulse. Combine Eq. (6) and Eq. (7) to obtain the echo model of point target as.

$$S_r(t,s) = \sigma \cdot rect(\frac{t - 2R(s)/C}{Tt}) \exp[j\pi K_t (t - 2R(s)/C)^2]$$
$$\cdot rect(\frac{s}{T_s}) \exp[-j\frac{4\pi}{\lambda} R(s)] \tag{8}$$

Where $R(s)$ represents the distance between the radar and the target, s is slow time in azimuth. The first index term is the chirp component, which determines the resolution in the range direction, and the second index term is the doppler component, which determines the resolution in the azimuth direction. There are many algorithms for echo processing. Among them, the BP (back projection) algorithm divides the echo data into two dimensions: range and azimuth. The range migration is corrected after range pulse compression, and then the azimuth pulse compression is performed to get high-resolution images. After two-dimension pulse compression, the ideal imaging response without the ionosphere is the *sinc* function shown below.

$$S_r(t,s) = \mathrm{sinc}\left[B \cdot \left(t - \frac{2R_0}{c}\right)\right] \mathrm{sinc}\left[|K_s T_s| s\right]$$
$$\cdot \exp\left(-\frac{j4\pi f_0 R_0}{c}\right) \tag{9}$$

Where R_0 is the vertical slant distance from target to radar. Eq. (5) shows that the additional phase of the ionosphere is related to frequency, so the electromagnetic waves passing through the Martian ionosphere will add different phase in the frequency domain. In the following, the first three terms $\Delta\phi_1(f), \Delta\phi_2(f), \Delta\phi_3(f)$ of Taylor expansion are main considered.

The signal is divided into range and azimuth to be processed separately. First, the range time t is Fourier transformed into f, substitute the linear term $\Delta\phi_1(f)$ into it, the range of the echo adds a phase term to the frequency domain expression.

$$S_{r\_\Delta q}(f,s) = \mathrm{rect}\left[\frac{f}{B}\right] \mathrm{rect}\left[\frac{s}{T_s}\right] \exp\left(-j\pi\frac{f}{K_t}\right)$$
$$\exp\left(-j\Delta\phi_1(f)\right) \exp\left(-\frac{j4\pi f_0 R(s)}{c}\right) \exp\left(-j2\pi f \cdot \frac{2R(s)}{c}\right) \tag{10}$$

After matched filtering for above signal, the FFT is performed to obtain the echo signal under the influence of the primary phase of the ionosphere as follows.

$$S_{r\_\Delta\phi}(t,s) \approx \mathrm{sinc}\left[B \cdot \left(t - \frac{2R(s)}{c} - \frac{2A \cdot TEC}{cf_0^2}\right)\right]$$
$$\cdot \mathrm{rect}\left[\frac{s}{T_s}\right] \exp\left(-j\pi\frac{2V^2}{\lambda R_0} s^2\right) \tag{11}$$

It can be seen that the time domain point target has shifted upward in the distance, and the offset is related with TEC and carrier frequency.

$$\Delta L_r = \frac{2A \cdot TEC}{cf_0^2} \cdot \frac{c}{2} = \frac{A \cdot TEC}{f_0^2} \tag{12}$$

The secondary phase effect is caused by the frequency quadratic function $\Delta\phi_2(f)$ in the Taylor expansion, this term is included the frequency domain echo signal can be expressed as.

$$S_{r\_\Delta\phi_2}(f,s) = \mathrm{rect}\left[\frac{f}{B}\right]\mathrm{rect}\left[\frac{s}{T_s}\right]\exp\left(-j\pi\frac{f^2}{K_t}\right)$$
$$\exp\left(-\Delta\phi_2(f)\right)\exp\left(-\frac{j4\pi f_0 R(s)}{c}\right)\exp\left(-j2\pi f\cdot\frac{2R(s)}{c}\right) \quad (13)$$

According to the principle of stationary phase, the transformation of the quadratic term $\Delta\phi_2(f)$ from frequency domain to time domain is the first term. Therefore, this term will cause the mismatch of the matched filtering in the range and cause the main lobe of the *sinc* function to expand. The quadratic phase error (QPE) is defined to measure the degree of mismatch, it is expressed with carrier frequency, total electron quantity, and bandwidth.

$$\mathrm{QPE} \approx \frac{\pi AB^2 TEC}{cf_0^3} \quad (14)$$

Similarly, the cubic phase error is the third term of frequency, and additional time quadratic function is introduced in the time domain. This phase error will increase the side lobe of the *sinc* function and cause the image to blur. The cubic phase error (CPE) is defined to measure the influence of the cubic term.

$$\mathrm{CPE} = \frac{\pi AB^3 TEC}{4cf_0^4} \quad (15)$$

3 Simulation of the impact of the Martian ionosphere on Tianwen 1 Paper Content

The Tianwen 1 orbiter subsurface investigation radar has two working frequency bands, 10-20MHz and 30-50MHz. The wider the bandwidth, the greater the difference between low-frequency and high-frequency components affected by the Martian ionosphere, so the simulation signal bandwidth is set to 20MHz. The carrier frequency is 0.4GHz and center frequency is 0.41GHz. The ionosphere of Mars is much thinner than that of the earth, the TEC is about one fifty of the earth [6]. So set the TEC=10TECU (1TECU= $10^{16}e$). For a point target, suppose its RCS=1. First, a one-dimensional simulation is performed to simulate the effects of the primary, secondary, and tertiary terms on echo pulse compression. Fig. 1 is the simulation result under the above parameters. Black, red, blue, and green curves represent the ideal signal, linear term, quadratic term and cubic term, respectively. Fig. 2 is the simulation result with increased TEC (20TECU).

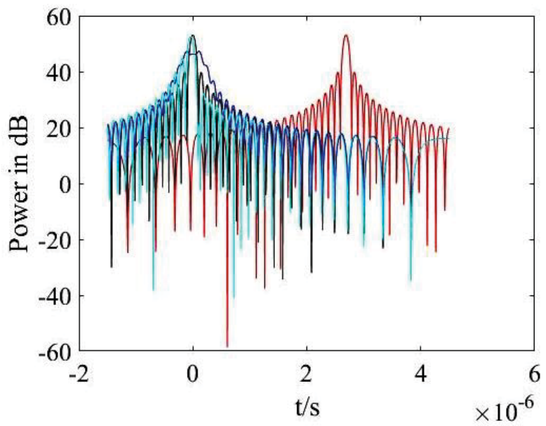

Fig. 1 Comparison of the influence of different phase items on the echo signal under 10TECU, black, red blue and green represents ideal signal, linear phase term, quadratic phase term and cubic phase term respectively

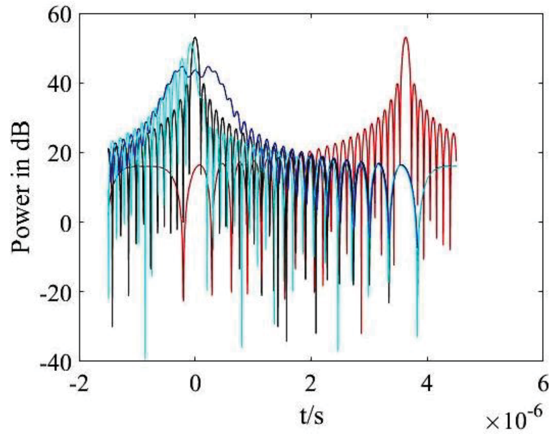

Fig. 2 Comparison of the influence of different phase items on the echo signal under 20TECU

It can be seen from the results that the ideal chirp signal is a *sinc* function after pulse compression. The primary phase term of the ionosphere will cause the image translation, and the secondary phase term will cause the image to defocus. The cubic phase term will cause the image side lobes to become larger. The larger the TEC, the more serious image position distortion and defocusing.

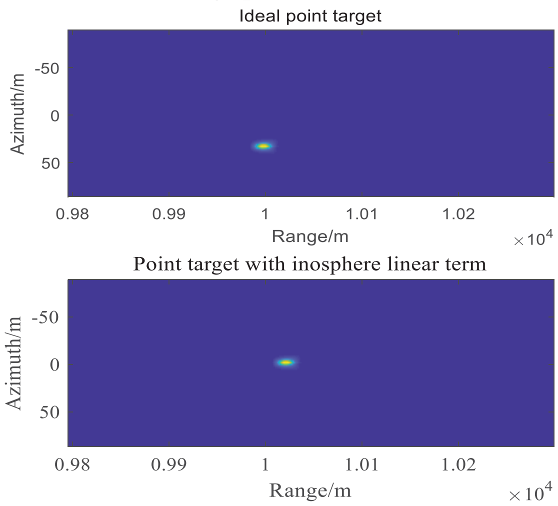

(a)

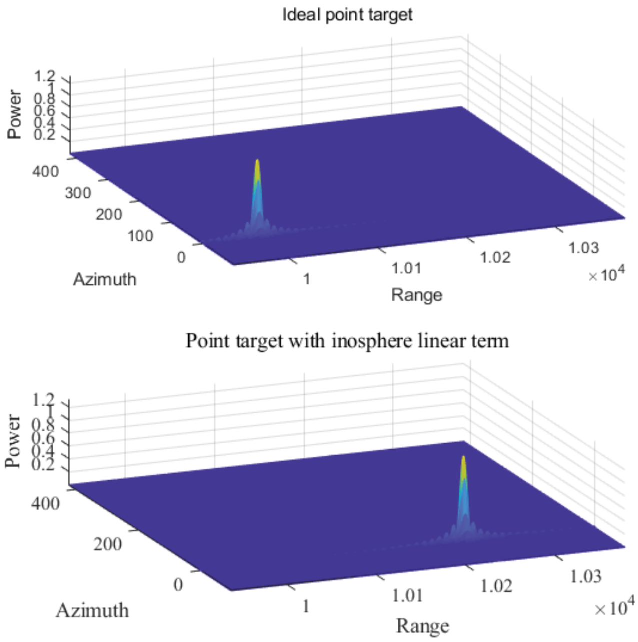

(b)

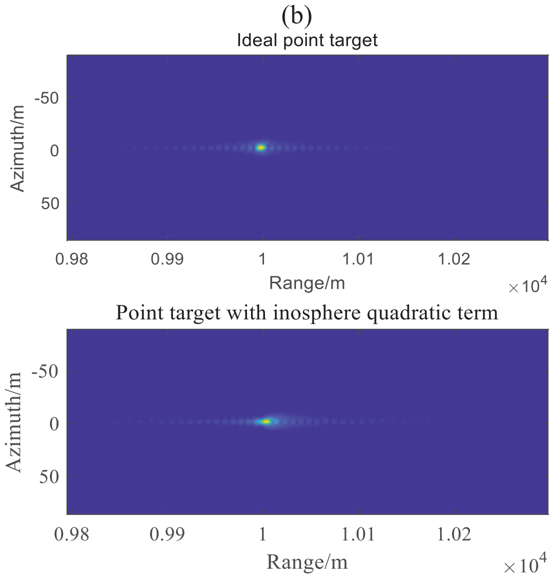

(c)

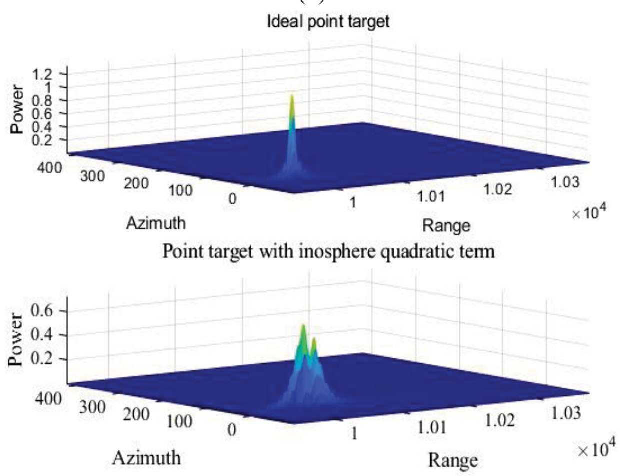

(d)

Fig. 3 Two-dimensional simulation of the point target in based on the ionosphere of Mars, Fig. (a) and (b) show the displacement of the point target due to the influence of the ionospheric primary term, Fig. (c) and (d) show the defocus of the point target due to the influence of the ionospheric quadratic term

From the simulation results, it can be calculated that when the bandwidth is 20MHz, carrier frequency is 0.4GHz, and TEC=10TECU (1TECU=$10^{16}e$), the target will be offset by about 23.96 meters from Eq. (16). Due to the influence of the ionosphere. And the point target is seriously defocused, causing the image resolution to drop.

$$\Delta L_r = \frac{A \cdot TEC}{f_0^2} = \frac{40.28 \times 10 \times 10^{16}}{(0.41 \times 10^9)^2} m = 23.96m \qquad (16)$$

4 Conclusion

This paper analyzes the image distortion caused by the interference of Martian ionosphere when the orbital subsurface detection radar on Tianwen 1 mission. From the results, it can be seen that the echo shifts and defocus due to different frequency components passing through the ionospheric group with different refractive indices. The shift amount reaches tens of meters, and severe image defocus appear. The linear, quadratic and cubic terms of the additional phase of the stationary ionosphere will only affect the range of the point target.

References

[1] Perminov V G. “The difficult road to Mars: a brief history of Mars exploration in the Soviet Union,” *National Aeronau- tics and Space Administration Headquarters*, 1999.

[2] Orosei R, Jordan R L, Morgan D D, et al. “Mars Advanced Radar for Subsurface and Ionospheric Sounding (MARSIS) after nine years of operation: A summary,” *Planetary and Space Science*, 2015, 112: 98-114.

[3] Restano M, Seu R, Picardi G. “A phase-gradient-autofocus algorithm for the recovery of marsis subsurface data,” *IEEE Geoscience and Remote Sensing Letters*, 2016, 13(6): 806-810.

[4] Gurnett, D., etal. (2005), “Radar soundings of the ionosphere of Mars,” *Science*, 310(5756), 1929-1933.

[5] Wang C, Zhang M, Xu ZW, etal. “Effects of Anisotropic Ionospheric Irregularities on Space-Bome SAR Imaging,” *IEEE Trans.Antennas Propagt.*, 2014, 62(9): 4664-4673.

[6] Cui, J., Galand, M., Yelle, R. V., Wei, Y., & Zhang, S.-J. “Day-to-night transport in the Martian ionosphere: Implications from total electron content measurements,” *Journal of Geophysical Research: Space Physics*, 2015, 120(3), 2333–2346.